Extended Abstracts of the 2012 International Conference on Solid State Devices and Materials, Kyoto, 2012, pp616-617

Low power and improved switching properties of selector-less Ta_2O_5 based ReRAM using Ti-rich TiN electrode

Beomyong Kim[1], Wangee Kim[1], Hyojune Kim[1], Kyooho Jung[1], Wooyoung Park[1], Bomin Seo[1], Moonsig Joo[1], Keejeung Lee[1], Kwon Hong[1], and Sungki Park[1]

[1]NM material Research Team, R&D Division, SK Hynix Semiconductor Inc.,
2091, Gyeongchung-daero, Bubal-eub, Icheon-si, Gyeonggi-do, Korea
Tel) +82-32-639-1261, Fax) +82-31-645-8139, E-mail) beomyong.kim@skhynix.com

1. Introduction

ReRAM without selector is essentially desirable compared to other types such as 1D1R, and 1T1R because of high scalability and its simplicity in process. Thus, from that point of view, it is imperative to achieve good switching properties with high non-linearity in selector-less ReRAM. However, non-linearity, On/Off ratio, and operation voltage are complicatedly entangled in tradeoff relationship. In this study, we investigated the effect of non-stoichiometric TiN top electrode on switching behaviors and non-linearity properties of Ta_2O_5 based ReRAM. As a result, thermodynamic approach has been made in explaining improvement of the amount of oxygen vacancies as well as the change in operation voltage with respect to Ti/N ratio has been scrutinized by measurement of the workfunction of the top electrodes.

2. Experimental

The structures of Top electrode (TE) TiN/TiO_x/Ta_2O_5/Bottom electrode (BE) TiN were fabricated using 50nm standard CMOS process. TE TiN was deposited by PVD by controlling N_2 flow during deposition to modulate the ratio of Ti to N, as summarized in Fig. 1(a). There are three groups of the stacks having the ratio of (A) 1.0, (B) 1.5, and (C) 4.0. The non-linearity factor (K_W) is defined as the ratio of I @ V_{set} to I @ $1/2V_{set}$ as formulated in Fig. 1(b). Finally, electrical switching characteristics were measured by current-voltage (I-V) sweep in DC and the workfunctions (WFs) of the electrodes were precisely analyzed by Ultraviolet Photoelectron Spectroscopy. In addition, X-ray photoelectron spectroscopy (XPS) allows measuring the change of oxygen vacancies in the reservoir.

3. Result and Discussion

Fig. 2 shows XPS Ti 2p spectra in both the (A) and (C) groups. For (C), the peak of Ti moves towards lower binding energy and TiO spectrum was detected, corresponding to increase of oxygen vacancies in TiO_x. To predict the redistribution of oxygen in Ti rich-TiN/TiO_x/Ta_2O_5 stack, the standard free energy in terms of the consumption of one mole of oxygen was compared for TiO, Ti_3O_5 and Ta_2O_5, as shown Fig. 3(a) [1]. During post-thermal process (< 320°C), TiO phase tends to form in the reaction between Ti in Ti-rich TiN and oxygen in Ti_3O_5. Thus, it is concluded that oxygen vacancy concentration in the reservoir TiO_x increases (Fig. 3(b)), which suggests that using reactive metals having high free energy is not suitable because oxygen atoms are strongly bonded to them [2]. In this case, Ta_2O_5 has higher free energy in comparison with TiO_x so that the Ta_2O_5 plays a dominant role in load resistance.

WF and sheet resistance (Rs) are shown as a function of the Ti/N ratio in Fig. 4. With increase in Ti content, WF is on decrease whereas Rs increases. The initial resistance decreases with increase in the Ti/N ratio, as shown in Fig. 5., which clearly indicates that Ti-rich TiN having low WF can greatly enhance Ohmic contact at the interface despite the small increment in resistance of the metal.

Fig. 6 shows I-V switching characteristics under the compliance current of 50μA for the various groups, (A), (B), (C), and Ti. It should be pointed out that as the Ti/N ratio increases, higher On/Off ratio was obtained without noticeable degradation of Kw, as illustrated in Fig. 7. These results in turn confirm the idea that enough amount of oxygen vacancies was generated by utilizing Ti-rich TiN. On the other hand, in the case of Ti electrode, switching properties were rapidly degraded over cycles (Fig. 6(d)). This stems from the fact that excessive amount of Ti diffuses into TiO_x/Ta_2O_5 stacks (not shown), making the level of current high.

Fig. 8 shows that the set voltage (V_{set}) reduces with the increase of Ti/N ratio, which is equivalent to low V_{set} being beneficial for low power operation. Fig. 9 is the cumulative graph of high resistance state (HRS) and low resistance state (LRS) currents for (A) and (C) groups, showing that the increment of LRS current is larger than that of HRS current. Linear fitting of 5th cycle of switching I-V for (C) was performed as given in Fig. 10. Both the HRS and LRS show the transition from direct tunneling to FN tunneling as voltage goes high, like the analogy in thin dielectric films, which is the direct evidence that On/Off ratio was improved while maintaining Kw value at the level of (A) (Fig. 7).

The switching mechanism of the TiO_x/Ta_2O_5 stack can be explained by the combination of filament and interface. (Fig. 11). Fig. 12 gives schematic band diagrams of (A) and (C) in LRS. The resistor structure in (C) has a good endurance property that shows no degradation up to 8,000 cycle and 12 hour retention at 150 ^{o}C (Fig.13).

4. Conclusion

We have successfully demonstrated the improved switching behaviors in TE Ti-rich TiN/TiO_x/Ta_2O_5/BE TiN stacks using 50nm tech node. Systematic data have been given to verify the combination of filament formation and redox reaction in switching operation. It has been proven that Ti-rich TiN allows a boost in On/Off ratio and operation voltage scaling without loss of Kw, which makes this Ti-rich TiN promising for future selector-less ReRAM applications.

References

[1] M. W. Chase et al., J. Phys. Chem. Ref. Data, **14** (1975)
[2] X. P. Wang et al., VLSI Tech. Dig., 2010

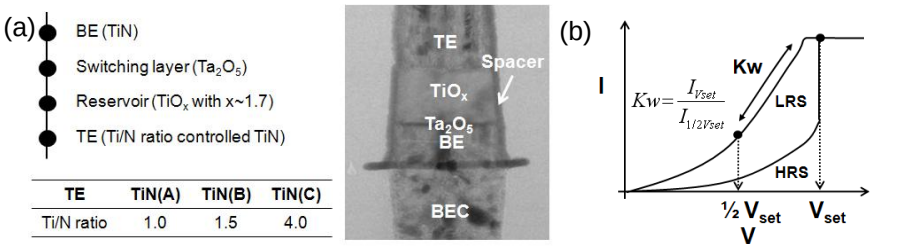

TE	TiN(A)	TiN(B)	TiN(C)
Ti/N ratio	1.0	1.5	4.0

Fig. 1 (a) Process flow of the fabricated ReRAM structure (b) definition of non-linearity (Kw)

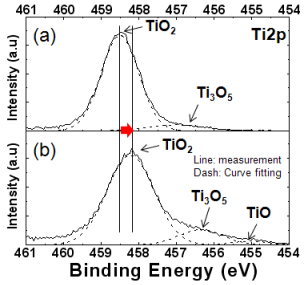

Fig. 2 XPS Ti2p spectra of TiO_x structures. (a) TiN(A), (b) TiN(C). (Sample preparation: TiN/TiOx was formed, and then TiN was selectively removed)

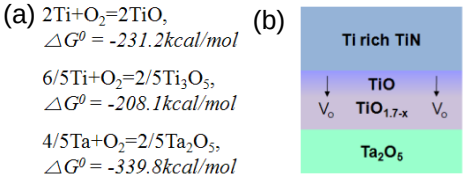

Fig. 3 (a) The standard free energy at 600K in terms of the consumption of one mole of oxygen for TiO, Ti_3O_5 and Ta_2O_5 (b) the schematic diagram for the high concentration of oxygen vacancy formation in TiO_x using Ti rich TiN.

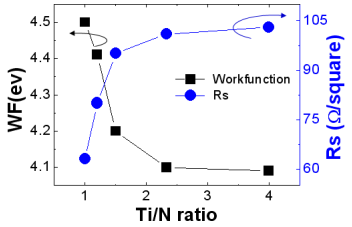

Fig. 4 WF and Rs as a function of Ti/N ratio.

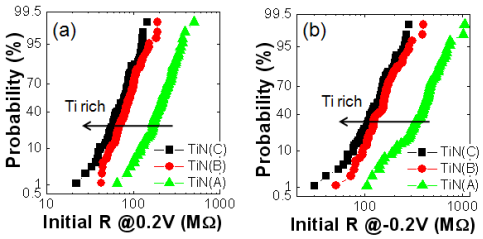

Fig. 5 The initial resistance of TiN(A), TiN(B) and TiN(C) at (a) 0.2V and (b) -0.2V.

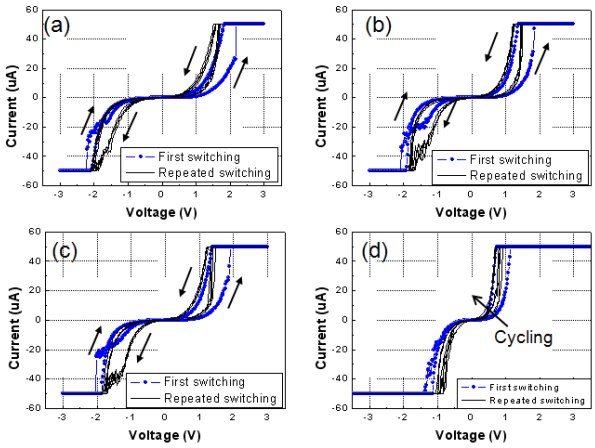

Fig. 6 DC I-V switching results for various TE electrodes. (a) TiN(A), (b) TiN(B), (c) TiN(C) and (d) Ti.

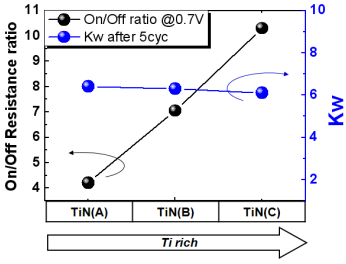

Fig. 7 Summary of On/Off ratio and Kw for TiN(A), TiN(B) and TiN(C). Kw was measured after 5th cycling.

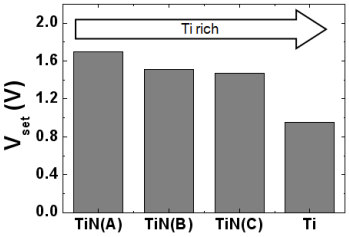

Fig. 8 Set voltage at 5th cycle of switching for TiN(A), TiN(B), TiN(C) and Ti.

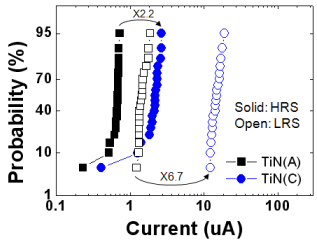

Fig. 9 Cumulative graph of HRS and LRS current for (a) TiN(A) and (b) TiN(C) resistor stacks.

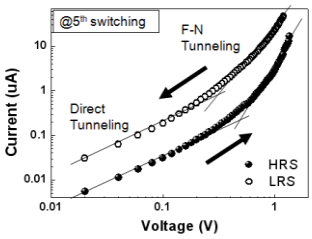

Fig. 10 Transition from direct tunneling to FN tunneling with voltage.

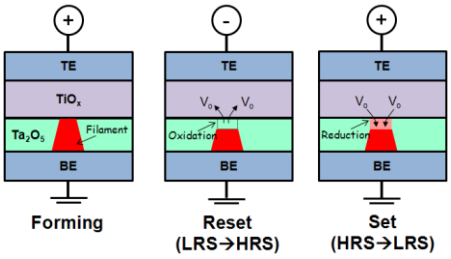

Fig. 11 Switching mechanism of TiOx/Ta_2O_5 stacks, combination of filament and interface.

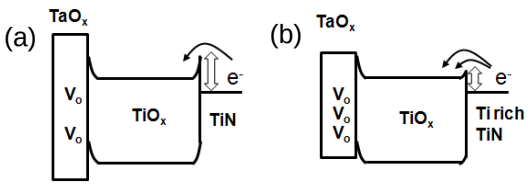

Fig. 12 Schematic band diagram of (a) TiN(A) and (b) TiN(C) stack in LRS.

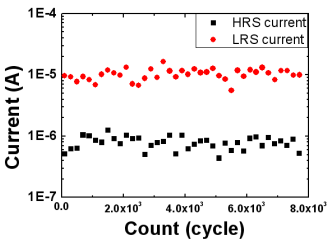

Fig.13 DC sweep switching endurance characteristics.

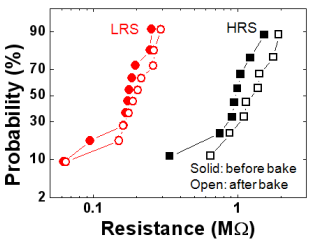

Fig.14 Retention property at 150°C for 12hr